Contribution of turbidimetry on the characterization of cement pastes bleeding

Author 1

- Youssef EL BITOURI, Associate professor
- LMGC, IMT Mines Ales, Univ Montpellier, CNRS, Ales, France
- ORCID number : 0000-0001-6284-299X

Author 2

- Nathalie Azéma, Professor
- LMGC, IMT Mines Ales, Univ Montpellier, CNRS, Ales, France
- ORCID number

Full contact details of corresponding author:

Name : Youssef El Bitouri

E-mail adress: **youssef.elbitouri@mines-ales.fr**

Full postal address: IMT Mines Alès, 6 Avenue de Clavières, 30100 Alès. France

Tel: +33-4-66-78-53-67

Abstract

The aim of this paper is to examine the contribution of turbidimetry measurements on the characterization of cement pastes bleeding. In some cases (e.g. presence of superplasticizer), the bleed water becomes turbid due to finest particles dispersion and the boundary between the bleed water and the consolidated paste becomes difficult to detect. Turbiscan device allows detecting this boundary more accurately than traditional tests. The role of superplasticizer and solid volume fraction on bleeding is examined. The bleeding measurements highlight the role of superplasticizer on bleeding and its kinetics. The effect of superplasticizer may be explained by better dispersion leading to release of water trapped between agglomerates. Furthermore, the existence of critical volume fraction, above which no bleeding occurs, close to that corresponding to the appearance of contacts between particles is shown. Finally, using rheological measurements, the correlation between the yield stress and bleeding has been possible.

Keywords

Bleeding; Cement paste, Settlement, Yield stress, Superplasticizer

1. Introduction

Stability of concentrated mineral suspensions must be well controlled and is of great importance in several domains as ceramics, covering industry, paper industry… notably cement and concrete. For the latter, comprehension of fresh state behavior of cement based materials allowed manufacturing special concretes such as self-compacting concretes (SCC) (Gaimster and Dixon, 2003; Okamura and Ozawa, 1996; Shi et al., 2015) and high performance concretes (HPC). In practice, fresh concrete should be quite fluid and resistant to instability phenomena (Kovler and Roussel, 2011; Navarrete and Lopez, 2017). A fluid concrete would be more sensitive to instability such as segregation and bleeding. Furthermore, it is well known that the fresh state of concrete affects strongly its strength and durability. For instance, excessive bleeding weakens the bond between cement matrix and aggregates and induces a heterogeneity of strength (Josserand et al., 2006). The bleeding can also cause major disorders, in particular for cementitious post-tensioning tendon grout. The European standard EN 447 limits the bleeding of these grouts to 0.3% after 3 hours at rest. Despite its negative consequences, mild bleeding can ensure a wet curing of concrete which limits the effects of drying shrinkage.

At the cement paste scale, bleeding occurs due to the difference between density of cement particles and water. It usually corresponds to the accumulation of clear water at the surface (Josserand et al., 2006; Kovler and Roussel, 2011; Perrot et al., 2012). Gravity is the driving force at the origin of bleeding. It induces the settlement of the solid particles causing in turn the upward displacement of water. Bleeding can thus be described as a settlement and consolidation process governing by the permeability of the network of interacting particles (Josserand et al., 2006). Powers (Powers, 1968) considered bleeding as a special case of sedimentation and described it by a general law derived from Poiseuille's law of capillary flow. He proposed a relation which can assess the initial bleeding rate as a function of solid volume fraction (Powers, 1968). The bleeding rate can be assumed to follow the Kozeny-Carman equation (Powers and Dahl, 1939), but Peng et al. (Peng et al., 2017) showed that this is not relevant since bleeding rate is not constant. In a recent study, Massoussi et al. (2017) suggest that bleeding cannot be simply described by a consolidation process, but is of obvious heterogeneous nature leading to the formation of preferential water extraction channels

(Massoussi et al., 2017). By using numerical image acquisition, Massoussi et al. (2017) showed that the bleeding process is composed of five stages: the induction period, the accelerating regime, the constant water extraction rate period, the consolidation regime and the final consolidated state. In their study, the effect of superplasticizer has not been examined.

In general, sedimentation in suspensions can be defined as the downward displacement of particles and depends mainly on particle size, density, and surface properties (Autier et al., 2014; Eckert et al., 1996). However, depending on solid volume fraction, there are different types of sedimentation. The extreme situations occur for very low volume fraction (diluted suspension) in which unit particles and agglomerates can settle independently, and for high volume fraction in which particles can interact (interparticle forces and direct contacts) forming a network that consolidate under its own-weight. Bleeding thus occurs when this network of interacting particles exists. In this case, in addition to sediment layer, a sharp front of a clear supernatant layer appears and increases over time (bleeding layer). In the case of suspension with superplasticizer, due to the dispersion of finest particles and the decrease of magnitude of interparticle forces, different zones can be observed: a turbid supernatant (turbid bleeding) containing finest particles which settle very slowly, and sediment with one or several zones with various concentrations. Whatever the mode of sedimentation, the suspension at the equilibrium is composed of a layer of more or less clear supernatant above a consolidating sediment (Eckert et al., 1996; Fitch, 1983; Peng et al., 2017). In this study, the bleeding corresponds to the supernatant layer forming above compact sediment, even for cement paste with low solid volume fractions.

There are several methods to measure bleeding such as those defined in the standards (EN 447, ASTM C243, ASTM C1741-18, ASTM C940 - 98a). However, the majority of these methods are difficult to use without a sharp bleeding front (Josserand and De Larrard, 2004; Massoussi et al., 2017; Radocea, 1992). For instance, methods based on the visual measurement of bleeding thickness cannot be used without a clear bleeding front. Another test based on the measurement of hydrostatic pressure (HYSPT) allow bleeding rate to be measured, but by assuming sharp bleeding front and homogeneous zone below bleed water (Peng and Jacobsen, 2013). Furthermore, Peng et al. (Peng et al., 2017) found that the bleeding rate of fresh cement paste determined by the Kozeny-Carman equation (Powers,

1968) and visual measurements remains constant whatever the water to cement ratio and the bleeding step. Josserand and de Larrard (Josserand and De Larrard, 2004) proposed a method which consists in sucking bleed water with pipette, but this method is more suitable for concrete than for cement pastes.

It thus appears that conventional bleeding tests are not always suitable for accurately measuring bleeding, especially when the latter is turbid. In addition, the incorrect determination of the bleeding could lead to false interpretations. In fact, Daczko (Daczko, 2012) reported that the absence of sharp bleeding front (e.g. turbid bleeding) does not guarantee that a mixture is stable. Test based on turbidity measurement could make it possible to measure the evolution of turbid bleeding more accurately than conventional tests (Peng et al., 2017). In fact, the Turbiscan device is able to detect nascent destabilization phenomenon in concentrated suspensions much faster than visual testing.

Furthermore, it appears that bleeding is related to rheological properties of the paste at rest. For instance, the self-compacting concrete is able to flow under its own-weight and can stay homogeneous. The first property is related to the stress required to initiate flow, i.e the yield stress, while the second involves the resistance of particles to bleeding and segregation. In addition, instabilities at rest occurs when the yield stress of suspending matrix is not sufficient to stabilize the particles (Roussel, 2006). It thus appears that yield stress and bleeding are two properties closely related. Attempts to correlate yield stress and bleeding can be found in the literature (El Bitouri and Azéma, 2021; Perrot et al., 2012). Perrot et al. (Perrot et al., 2012) found that this correlation is indirect and difficult to use in practice. They based their conclusion on the fact that at the critical water to cement ratio below which no bleeding occurs, the cement paste without SP displayed a yield stress of about 300 Pa, while cement paste with 3% of SP displayed a yield stress of 40 Pa. However, their study was based on visual observation with two measurement of bleeding at 1 and 2 hours, and turbid bleeding and the retarding effect of SP were not mentioned.

The yield stress takes its origins from direct contacts and interparticle forces which contribute to form an internal network of particles able to resist to applied stress (Dzuy and Boger, 2002; Roussel et al., 2010). The role of solid volume fraction on the yield stress is crucial and well documented in literature (Flatt, 2004; Flatt and Bowen, 2006; Mehdipour and Khayat, 2018;

Perrot et al., 2012; Toutou and Roussel, 2006; Zhou et al., 2002). Different critical volume fractions corresponding to the dominating physical phenomena are defined (Roussel et al., 2010). At rest, there is a volume fraction threshold below which cement paste doesn't display any yield stress. This threshold is known as percolation volume fraction (ϕ_{perc}) above which a network of interparticle forces appears in the material (Eckert et al., 1996; Roussel et al., 2010). In literature, the values of the percolation volume fraction are ranging from 0.2 to 0.4 (Flatt and Bowen, 2006; Perrot et al., 2012; Toutou and Roussel, 2006). Furthermore, it is well known that yield stress and viscosity diverges when solid volume fraction reaches a critical value (ϕ_{div}) (Roussel et al., 2010). The divergence of yield stress results from rigid contact between cement particles. It has to be kept in mind that this critical value is different from the maximum dense packing due to agglomeration of particles (Roussel et al., 2010). The addition of superplasticizer allows dispersing the agglomerates and thus to get closer to the real maximum packing (ϕ_m). Furthermore, it is shown that a transition volume fraction of the order of 0.8 ϕ_{div} separates suspensions in which the yield stress is mainly due to interparticle forces network and suspensions in which the yield stress is mainly due to a direct contacts network. Roussel et al. (Roussel et al., 2010) showed that below a percolation threshold (ϕ_{perc}), there are no direct contacts nor interparticle forces forming a network able to resist to applied stress, and thus, the cement paste doesn't display any yield stress. Also, in cement paste with volume fraction below the percolation threshold, cement particles can settle independently (hindered sedimentation). Above the percolation threshold, a network of interacting particles consolidates under its own weight, which corresponds to bleeding domain. From a critical solid volume fraction, bleeding becomes negligible (Perrot et al., 2012).

The aim of this paper is to examine the contribution of turbidimetry measurements on the characterization of cement pastes bleeding. The role of superplasticizer and solid volume fraction is examined. Since bleeding and yield stress originate from the same mechanisms, their correlation is also investigated. For this, rheological measurements are performed to examine the effect of superplasticizer and particle size on the different transition volume fractions: the percolation threshold (ϕ_{perc}), the transition volume fraction to frictional regime (0.8 ϕ_{div}), and the apparent dense packing (ϕ_{div}).

2. Materials and methods

2.1 Materials

The experiments were carried out by using cement (CEM II/A-L 42.5 N). Particle size distributions (in water) were determined by a laser granulometer S13320 from Beckman Coulter Company with an adapted optical model. As shown in Fig. 13, cement exhibited a broad particle size distribution ranging from 0.04 to 92.1 µm, with a main mode of about 17.30 µm.

A commercial polycarboxylate based superplasticizer with an equivalent dry extract content of 20 wt% is used.

2.2 Sample preparation

Cement pastes were mixed with deionized water in a planetary agitator according to the following sequence: 5 minutes mixing at 500 rpm, scraping the mixer walls to homogenize the mix (30 seconds), 5 minutes mixing at 500 rpm.

For cement pastes with superplasticizer, the binder and 90 wt% of the total water were mixed according to the following mixing procedure: 5 minutes mixing at 500 and scraping the mixer walls to homogenize the mix, 10 min resting. The superplasticizer and the remaining 10% of the water were then added to the mix which was mixed for 5 min at 500 rpm. Two dosage of superplasticizer were studied: 0.1 and 1 wt% of dry substance.

Cement pastes were prepared at the ambient temperature (22°C±2) with water to cement ratios (w/c) ranging from 0.2 to 1 which corresponds to solid volume fractions ranging from 0.24 to 0.56 (Table 5). The initial solid volume fraction is calculated according to:

$$\emptyset = (1 + \rho_c W/\rho_w C)^{-1} \quad (1)$$

Where : $\emptyset$ is the initial solid volume fraction, ρ_c and ρ_w are respectively the density of cement (3.14 g/cm²) and water, C and W are respectively the mass of cement and water.

All the tests were performed at the ambient temperature (22°C±2) during the dormant/induction period of cement hydration and hence changes due to chemical activity are not considered. The initial setting time measured by Vicat's needle in accordance with ASTM C191 standard in neat cement paste is of about 130 minutes. The addition of superplasticizer induces retarding effect leading to an increase of initial setting time.

2.3 Bleeding experiments

Bleeding measurements were carried out using an analyzer of concentrated suspensions, the Turbiscan LAB from Formulaction France. Turbiscan device consists of a vertical light scanner (near-infrared light source (λ=860 nm)) with backscattering and transmission sensors able to detect nascent destabilization phenomenon in concentrated suspensions (Mengual et al., 1999). The transmission sensor detects the light transmitted across the sample (at 0° from the incident beam), while the backscattered detector receives the light scattered backward by the sample (at 135° from the incident beam). The vertical scanner, which moves along the whole sample height (with a measuring step of 40µm), recorded the transmission (T) and backscattered (BS) profiles each 1 minute during the first hour and then each 5 min for the following 1 hour (Fig. 14). The rates of transmitted (*T)* and backscattered (*BS*) light are related to the solid volume fraction ϕ and the mean particles diameter *d* (Mengual et al., 1999) as follows :

$$\%\mathrm{T} \approx \exp\left(-\frac{A\emptyset}{d}\right) \tag{2}$$

$$\%\mathrm{BS} \approx \frac{B\emptyset}{d} \tag{3}$$

Where: A and B are constant parameters. Thus, changes in transmission (or/and backscattered) signal results from change in solid volume fraction and/or mean diameter.

Fig. 14 shows an example of sedimentation column with the recorded transmitted and backscattered signals. At the beginning of the experiment, the paste is opaque and there is zero transmission (x-axis) along the height of the cell (y-axis). With increasing time, a supernatant gradually forms at the top of the cell, characterized by an increase in transmission. The height of this supernatant corresponds to the bleeding layer. The evolution of bleeding front (boundary between the supernatant and the consolidated paste) can be characterized by the displacement of the transmission and backscattering signals (Fig. 14). The recorded profiles obtained by Turbiscan allow determining the bleeding layer, whether clear or turbid, more accurately than traditional bleeding test methods (Massoussi et al., 2017; Peng et al., 2017; Perrot et al., 2012). Moreover, Turbiscan allows quantifying the bleeding rate and solid volume fraction (and/or mean diameter) of each layer in the sedimentation column.

After mixing, a 55 mm height and 25 mm diameter cylindrical tube is filled with paste. The initial height of the paste is of 45 mm for all tests, corresponding to a volume of 27 ml. After filling, the

tube is immediately sealed to prevent water evaporation and introduced in the Turbiscan device. It is worth noting that the bleeding measurements could be affected by the wall effect. The diameter of the tube is large enough to limit the wall effect since the disturbed thickness is of few microns (Ben Aîm, 1970). Massoussi et al. (Massoussi et al., 2017) found that cement pastes bleeding is not affected by the presence of the interface between the material and the tube wall for diameter larger than 2.2 cm.

Bleeding is determined as the ratio of the height of the supernatant (transmission zone) $\mathrm{H_{sup}}$ to the initial height of the cement paste $\mathrm{H_c}$:

$$\mathrm{Bleeding\ (t)} = 100 \times \mathrm{H_{sup}}(t)/\mathrm{H_c} \quad (4)$$

2.4 Rheological measurements

Rheological measurements were carried out using an experimental Couette rheometer AR2000 ex from TA instruments equipped with a four blades vane geometry (internal diameter = 28 mm, the outer cup diameter = 30 mm). The geometry constants were calibrated using Couette analogy (Aït-kadi et al., 2002).

The performed measurement procedure consists of a stress growth experiment which allows measuring the static yield stress (Dzuy and Boger, 2002; Mahaut et al., 2008). The stress growth procedure starts with a strong pre-shear (100 s^{-1} during 200 s) followed by a resting time of 200 s, and then a small rotational velocity corresponding to a shear rate of 10^{-2} s^{-1} is applied to the vane geometry. On the shear rate vs. strain curve obtained for yield stress measurement (Fig. 15), the stress begins to increase linearly with the strain to reach a peak followed by a steady state flow. The peak defines the static yield stress which corresponds to the minimum stress to induce flow.

3. Results

3.1 Effect of solid volume fraction on bleeding

The evolution of bleeding as a function of water to cement ratio (and corresponding volume fraction) is shown in Fig. 16. This evolution consists of two stages. In the first stage, bleeding increases linearly with time. The slope of this linear zone defines bleeding rate. Above this linear zone, bleeding reaches a plateau (bleeding capacity). It can be observed that bleeding reaches a steady state before 2 hours (consolidation regime). Beyond this time, the contribution of

hydration reactions on the stabilization of the cement paste is not negligible (setting time). The bleeding capacity corresponds thus to the value of bleeding reached at 2 hours.

The evolution of bleeding capacity and its rate as a function of solid volume fraction is shown in Fig. 17. It can be noted that both the bleeding and its rate decrease with the increase of solid volume fraction. For low solid volume fractions, which correspond in practice to that of cement grouts, bleeding capacity is high. It has to be kept in mind, that bleeding less than 5% is considered as acceptable in such materials (Azadi et al., 2017). The bleeding of cement grout is reduced by the addition of others components (e.g. bentonite).

From solid volume fraction of 0.35, the bleeding is less than 5% and becomes negligible at 0.44. This volume fraction domain corresponds to standard water to cement ratio in concretes.

3.2 Effect of superplasticizer on bleeding

The effect of superplasticizer on bleeding is illustrated in Fig. 17 and Fig. 18. It appears that bleeding and its rate increase with the increase of superplasticizer dosage. However, the time required to reach the plateau increases with increasing superplasticizer dosage.

It thus seems that the addition of superplasticizer (with the studied dosages) leads to an increase of both bleeding capacity and bleeding rate, but also the time required to reach the plateau. This effect may be explained in part by a change in the cement particles assembly since the addition of superplasticizer allows a better dispersion of the cement particles. The permeability of solid skeleton is thus expected to increase. However, Perrot et al. (Perrot et al., 2013) found that the addition of superplasticizer reduces the initial bleeding rate and increases bleeding capacity. They reported that the better dispersion of cement particles in the presence of superplasticizer induces a finer porous network that increases the flow resistance inside the material. They found that the permeability is decreased by about a decade and the bleeding rate is decreased by the same order of magnitude in the presence of superplasticizer (dosage between 0 and 3%). Caution should be exerted about the effect of superplasticizer on the permeability of fresh cement paste due to the complexity of measurement methods and the specificities of the porous medium (compressibility, hydration). Moreover, the apparent permeability of fresh cement paste is not constant and depends on the bleeding stage. Massoussi et al. (Massoussi et al., 2017) reported that during the accelerating period of bleeding, the apparent permeability of the paste increases due to the formation and percolation

of the water extraction channels. The effect of superplasticizer on the permeability of fresh cement paste remains misunderstood and requires more investigations.

Furthermore, the increase of bleeding and its rate in the presence of superplasticizer could be explained, in part, by a deagglomeration effect. In fact, the addition of superplasticizer allows a better dispersion of cement particles, releasing water trapped by agglomerates. It should be noted that the permeability and the deagglomeration effects could be probably linked which could leads to a localization effect (localized bleeding). More investigations are needed to clarify the mechanisms at the origins of increasing bleeding and its kinetics in the presence of superplasticizer.

The rate of excess water released (Fig. 18) due to the better dispersion of cement particles can be assessed and quantified, through the difference of the bleeding thicknesses at 2h (H_{sup}) between cement paste without superplasticizer and cement paste with 1% SP as follows:

$$\%Excess\ water = \left(\mathrm{H_{sup}}(SP = 1\%) - \mathrm{H_{sup}}(SP = 0\%)\right) \times A/V_i \quad (2)$$

Where: A is the area of the Turbiscan tube, V_i is the initial volume of water. The height of the column H_c is constant. The presence of finest particles in the supernatant is neglected.

Fig. 19 presents the rate of excess water extracted as a function of volume fraction. The excess water extracted represents between 12% and 2% of the initial water volume. It is interesting to note that this rate decreases with the increase of solid volume fraction. This indicates that the dispersion effect of superplasticizer is attenuated with the increase of solid volume fraction. In fact, when solid volume fraction reaches a high value, there is an appearance of direct contacts between cement particles which block the dispersive action produced by electrosteric effect. The latter is effective when the interparticle forces are the dominating physical phenomenon in the suspension. When contacts between particles appear, it is more difficult to disperse them. The network of cement particles is compact and the bleeding becomes negligible.

Superplasticizers can have a deleterious effect on bleeding. For example, with a water to cement ratio of 0.6, increasing the dosage of superplasticizer leads to a significant increase in bleeding as shown in Fig. 18. It should be noted that the use of superplasticizers is generally not necessary at such water to cement ratio. Furthermore, the water to cement ratio (and the corresponding volume fraction) from which the bleeding becomes negligible decreases

(increases) with the increase of the superplasticizer dosage (Fig. 17). Thus, the de-agglomeration effect, generally required to increase the workability of cementitious materials, can therefore prove to be deleterious for bleeding. When superplasticizer is employed, it is therefore important to determine the bleeding layer correctly. This is not always obvious, especially when the bleeding front is not sharp. The contribution of turbiscan device on the determination of the bleeding front is illustrated in Fig. 20 for cement paste with 0.1% SP (w/c=0.9). After 2 hours of settling, according to the transmitted signal (T), only a small bleeding layer is observed (peak between 42 and 44 mm). No transmission is observed in the rest of the column that remains turbid. However, a decrease of the backscattered signal (BS) is observed between 33 and 42 mm. The rate of backscattered signal remains constant after 2 hours between 0 and 33 mm. The decrease in the backscattered signal suggests a decrease of solid volume fraction (eq 3). The boundary of this layer with reduced volume fraction is not sharp and difficult to determine with some bleeding tests (e.g. visual observation in a graduated cylinder, numerical image acquisition). The real front of bleeding at 2 hours is located at 33mm as shown in Fig. 20. In order to confirm that this turbid layer can be considered as bleeding, some samples are left in the closed tube until hardened. As shown in Fig. 20, the turbid layer clarifies over time and its thickness little changes. The hardened paste located at the bottom of this layer presents different contrasts visible as a decrease in the backscattered rate.

3.3 Bleeding and yield stress

The yield stress measurements were performed to examine the effect of superplasticizer on transition volume fractions. As shown in Fig. 21, the yield stress increases with solid volume fraction ϕ. The percolation volume fraction, from which cement paste without superplasticizer exhibits a minimum stress, corresponds to 0.31. The addition of superplasticizer (SP) increases this percolation volume fraction (0.41 for 0.1% SP and 0.52 for 1% SP). In fact, in cement paste with superplasticizer, due to the dispersive action by electrosteric effect, it is more difficult to form a percolated network of particles.

Furthermore, the value of ϕ_{div} can be derived from experimental data by plotting the asymptote of the curve presented in Fig. 21. The solid volume fraction ϕ_{div}, for which yield stress diverges, is thus of about 0.56 for cement paste without superplasticizer. It depends on the agglomeration

state of the suspension since it increases with the incorporation of superplasticizer (0.59 for 0.1% SP and 0.61 for 1% SP).

The measured static yield stresses can be fitted by the following relationship (represented by the dotted lines in Fig. 21) derived from the YODEL (Yield stress mODEL)(Flatt and Bowen, 2006):

$$\tau_0 \cong k \frac{\emptyset^2(\emptyset - \emptyset_{perc})}{\emptyset_{div}(\emptyset_{div} - \emptyset)} \quad (2)$$

Where: k is a fitting parameter (Table 3), $\emptyset$ is the solid volume fraction, $\emptyset_{perc}$ the percolation volume fraction and $\emptyset_{div}$ is the solid volume fraction for which the yield stress diverges.

As reported by Roussel et al. (Roussel et al., 2010), the solid volume fraction of 0.8 ϕ_{div} separates the suspensions in which the yield stress is mainly due to a network of interparticle forces and the suspensions in which the yield stress is mainly due to direct contacts network (Perrot et al., 2013; Roussel et al., 2010).

The transition volume fractions corresponding to the percolation threshold (ϕ_{perc}), the appearance of contacts (0.8 ϕ_{div}), and the apparent dense packing (ϕ_{div}) are plotted as a function of superplasticizer dosage (Fig. 22). These critical volume fractions allow assessing the dominating physical phenomenon as reported by Roussel et al. (Roussel et al., 2010).

Below the percolation threshold, the interparticle forces are not able to maintain particles in suspension. The settling of cement particles can be described by hindered sedimentation. From the percolation threshold, the magnitude of interparticle forces increases leading to the formation of a network of particles able to withstand a stress. This network consolidates under its own weight leading to the bleeding. When the contacts appear, the network of cement particles is compact and the bleeding becomes negligible.

It is interesting to note that the addition of superplasticizer leads to an increase of transition volume fractions. The domain in which the interparticle forces are the dominating phenomenon is thus reduced with the increase of superplasticizer dosage. It is the same case for the domain in which the contacts are predominant (Fig. 22).

Since the yield stress and bleeding originate from the network of interacting particles, their correlation seems to be possible and interesting from a practical point of view. Fig. 23 shows the yield stress and the bleeding as a function of solid volume fraction. It can be noted that the

critical solid volume fraction above which no bleeding occurs (ϕ_c) is different from the percolation threshold (ϕ_{perc}). The bleeding phenomenon concerns suspensions in which a network of interacting particles exists. Below the percolation threshold, bleeding is important while the yield stress is negligible. Bleeding becomes negligible and yield stress diverges when solid volume fraction is close to that corresponding to the appearance of the contacts between cement particles (0.8 ϕ_{div}). In fact, from this solid volume fraction, the appearance of rigid contacts between particles leads to a compact network. The percolation of the low amount of water available becomes difficult, and the fresh cement paste thus remains homogeneous and cannot bleed.

Furthermore, there is a minimum yield stress above which no bleeding occurs. This minimum yield stress of about 10 Pa does not depend on the superplasticizer dosage as shown in Fig. 23. Fig. 24 presents the correlation between yield stress and bleeding. Two extreme domains can be observed. The first domain corresponds to a negligible bleeding with a high yield stress and the second domain corresponds to a negligible yield stress and an important bleeding. These two domains are not of interest for cementitious materials, since a high yield stress does not allow sufficient workability to be obtained, and significant bleeding can have deleterious consequences. Between these domains, yield stress and bleeding seem to be correlated and this correlation does not depend on the superplasticizer dosage. This domain is of interest for cementitious materials since a compromise between workability and bleeding (stability) can be obtained. The yield stress is low enough to ensure workability, and high enough to limit bleeding.

4. Conclusions

The aim of this paper is to investigate the contribution of Turbiscan device on the characterization of mineral suspensions bleeding especially cement pastes bleeding compared to alumina suspensions. The effect of superplasticizer, solid volume fraction and particles size on bleeding is also examined. The main results of this paper are:

- The use of Turbiscan device allows turbid bleeding to be characterized more accurately than traditional tests, although no interface between the bleed water and the paste can be seen by visual observation.

- The use of superplasticizers leads to an increase in bleeding and its rate. This effect may be explained by particles dispersion which release water trapped beween agglomerates.
- Rheological measurements show that critical volume fractions depend on the superplasticizer dosage.
- A critical solid volume fraction (ϕ_c) above which no bleeding occurs is close to the transition volume fraction ($0.8\phi_{div}$) corresponding to the appearance of rigid contacts between particles. This critical volume fraction increases as a function of superplasticizer dosage.
- Correlation between yield stress and bleeding is possible. A minimum yield stress, not superplasticizer dosage dependent, above which no bleeding occurs is of about 10-50 Pa.

References

Aït-kadi, A., Marchal, P., Choplin, L., Bousmina, M., 2002. Quantitative Analysis of Mixer-Type Rheometers.

Autier, C., Azéma, N., Boustingorry, P., 2014. Using settling behaviour to study mesostructural organization of cement pastes and superplasticizer efficiency. Colloids Surfaces A Physicochem. Eng. Asp. 450, 36–45. https://doi.org/10.1016/j.colsurfa.2014.02.050

Azadi, M.R., Taghichian, A., Taheri, A., 2017. Optimization of cement-based grouts using chemical additives. J. Rock Mech. Geotech. Eng. https://doi.org/10.1016/j.jrmge.2016.11.013

Ben Aîm, R., 1970. Etude de la texture des empilements de grains. Application à la détermination de la perméabilité des mélanges binaires en régime moléculaire, intermédiaire, laminaire. Faculté des sciences de l'Université de Nancy.

Daczko, J.A., 2012. Self-consolidating concrete: Applying what we know, Self-Consolidating Concrete: Applying What We Know. https://doi.org/10.1201/b11721

Dzuy, N.Q., Boger, D. V., 2002. Direct Yield Stress Measurement with the Vane Method. J. Rheol. (N. Y. N. Y). https://doi.org/10.1122/1.549794

Eckert, W.F., Masliyah, J.H., Gray, M.R., Fedorak, P.M., 1996. Prediction of Sedimentation and Consolidation of Fine Tails. AIChE J. https://doi.org/10.1002/aic.690420409

El Bitouri, Y., Azéma, N., 2021. Potential Correlation Between Yield Stress and Bleeding. ACI Symp. Publ. 349.

Fitch, B., 1983. Kynch theory and compression zones. AIChE J. https://doi.org/10.1002/aic.690290611

Flatt, R.J., 2004. Dispersion forces in cement suspensions. Cem. Concr. Res. 34, 399–408. https://doi.org/10.1016/j.cemconres.2003.08.019

Flatt, R.J., Bowen, P., 2006. Yodel: A yield stress model for suspensions. J. Am. Ceram. Soc. 89, 1244–1256. https://doi.org/10.1111/j.1551-2916.2005.00888.x

Gaimster, R., Dixon, N., 2003. Self-compacting concrete, in: Advanced Concrete Technology. https://doi.org/10.1016/B978-075065686-3/50295-0

Josserand, L., Coussy, O., de Larrard, F., 2006. Bleeding of concrete as an ageing consolidation process. Cem. Concr. Res. https://doi.org/10.1016/j.cemconres.2004.10.006

Josserand, L., De Larrard, F., 2004. A method for concrete bleeding measurement. Mater. Struct. Constr. https://doi.org/10.1617/14052

Kovler, K., Roussel, N., 2011. Properties of fresh and hardened concrete. Cem. Concr. Res. https://doi.org/10.1016/j.cemconres.2011.03.009

Mahaut, F., Mokéddem, S., Chateau, X., Roussel, N., Ovarlez, G., 2008. Effect of coarse particle volume fraction on the yield stress and thixotropy of cementitious materials. Cem. Concr. Res. 38, 1276–1285. https://doi.org/10.1016/j.cemconres.2008.06.001

Massoussi, N., Keita, E., Roussel, N., 2017. The heterogeneous nature of bleeding in cement pastes. Cem. Concr. Res. https://doi.org/10.1016/j.cemconres.2017.02.012

Mehdipour, I., Khayat, K.H., 2018. Understanding the role of particle packing characteristics in rheo-physical properties of cementitious suspensions: A literature review. Constr. Build. Mater. https://doi.org/10.1016/j.conbuildmat.2017.11.147

Mengual, O., Meunier, G., Cayre, I., Puech, K., Snabre, P., 1999. Characterisation of instability of concentrated dispersions by a new optical analyser: The TURBISCAN MA 1000. Colloids Surfaces A Physicochem. Eng. Asp. 152, 111–123. https://doi.org/10.1016/S0927-7757(98)00680-3

Navarrete, I., Lopez, M., 2017. Understanding the relationship between the segregation of concrete and coarse aggregate density and size. Constr. Build. Mater.

https://doi.org/10.1016/j.conbuildmat.2017.05.185

Okamura, H., Ozawa, K., 1996. Self-compacting high performance concrete. Struct. Eng. Int. J. Int. Assoc. Bridg. Struct. Eng. https://doi.org/10.2749/101686696780496292

Peng, Y., Jacobsen, S., 2013. Influence of water/cement ratio, admixtures and filler on sedimentation and bleeding of cement paste. Cem. Concr. Res. https://doi.org/10.1016/j.cemconres.2013.09.003

Peng, Y., Lauten, R.A., Reknes, K., Jacobsen, S., 2017. Bleeding and sedimentation of cement paste measured by hydrostatic pressure and Turbiscan. Cem. Concr. Compos. 76, 25–38. https://doi.org/10.1016/j.cemconcomp.2016.11.013

Perrot, A., Lecompte, T., Khelifi, H., Brumaud, C., Hot, J., Roussel, N., 2012. Yield stress and bleeding of fresh cement pastes. Cem. Concr. Res. 42, 937–944. https://doi.org/10.1016/j.cemconres.2012.03.015

Perrot, A., Rangeard, D., Picandet, V., Mélinge, Y., 2013. Hydro-mechanical properties of fresh cement pastes containing polycarboxylate superplasticizer. Cem. Concr. Res. https://doi.org/10.1016/j.cemconres.2013.06.015

Powers, T.C., 1968. The properties of fresh concrete. J. Wiley Sons 533–652.

Powers, T.C., Dahl, L.A., 1939. The bleeding of Portland cement paste, mortar and concrete, treated as a special case of sedimentation,. Portland Cement Association Bulletin. No.2, Chicago.

Radocea, A., 1992. A new method for studying bleeding of cement paste. Cem. Concr. Res. https://doi.org/10.1016/0008-8846(92)90110-H

Roussel, N., 2006. Correlation between yield stress and slump: Comparison between numerical simulations and concrete rheometers results. Mater. Struct. Constr. https://doi.org/10.1617/s11527-005-9035-2

Roussel, N., Lemaître, A., Flatt, R.J., Coussot, P., 2010. Steady state flow of cement suspensions: A micromechanical state of the art. Cem. Concr. Res. 40, 77–84. https://doi.org/10.1016/j.cemconres.2009.08.026

Shi, C., Wu, Z., Lv, K., Wu, L., 2015. A review on mixture design methods for self-compacting concrete. Constr. Build. Mater. https://doi.org/10.1016/j.conbuildmat.2015.03.079

Toutou, Z., Roussel, N., 2006. Multi scale experimental study of concrete rheology: From water

scale to gravel scale. Mater. Struct. Constr. https://doi.org/10.1617/s11527-005-9047-y

Zhou, Z., Solomon, M.J., Scales, P.J., Boger, D. V., 2002. The yield stress of concentrated flocculated suspensions of size distributed particles. J. Rheol. (N. Y. N. Y). https://doi.org/10.1122/1.551029

Table 1. Granular and physical characteristics of cement

	cement
Measured density	3.14
specific surface (cm²/g)	3700 (Blaine)
Principal mode (µm)	22.73
dmean (µm)	17.30
dmin (µm)	0.04
dmax (µm)	92.09

Table 2. Water to cement ratios (w/c) used and the corresponding solid volume fractions

w/c ratio	solid volume fraction
0.25	0.56
0.3	0.52
0.35	0.48
0.4	0.44
0.45	0.41
0.5	0.39
0.6	0.35
0.7	0.31
0.8	0.28
0.9	0.26
1	0.24

Table 3. Parameters used to fit the experimental data

SP dosage (%)	0	0.1	1
percolation volume fraction ϕ_{perc}	0.31	0.42	0.52
maximum volume fraction ϕ_{div}	0.56	0.59	0.61
fitting parameter (k)	65	65	65

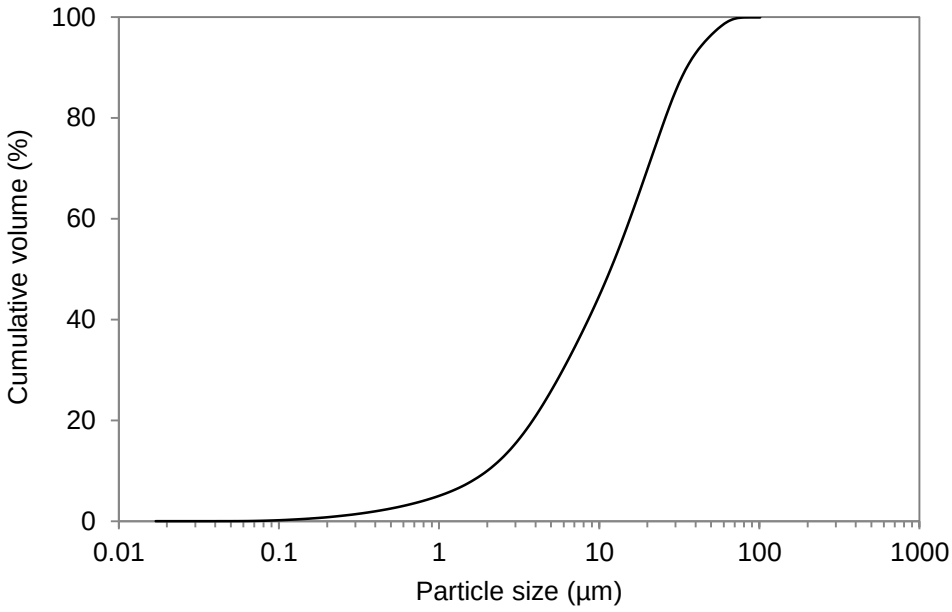

449
450

Fig. 1. Particle size distribution of cement

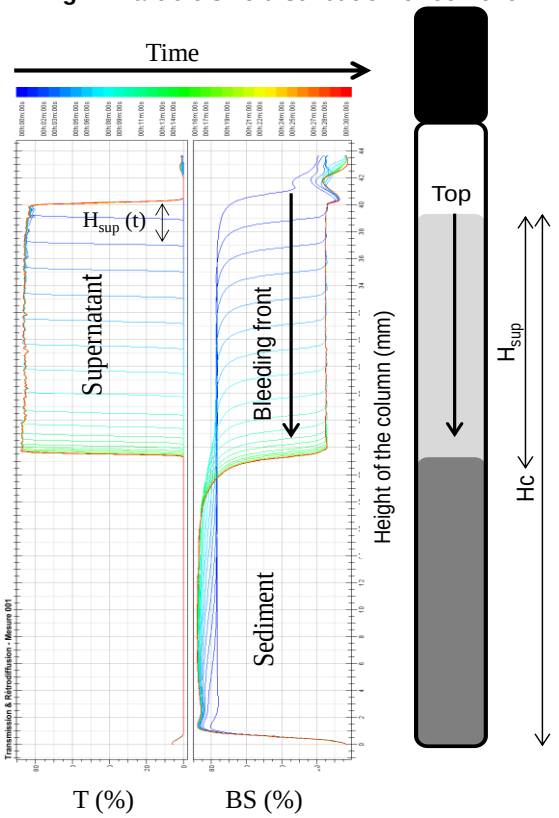

451
452

Fig. 2. Illustration of sedimentation column and transmission and backscattered patterns

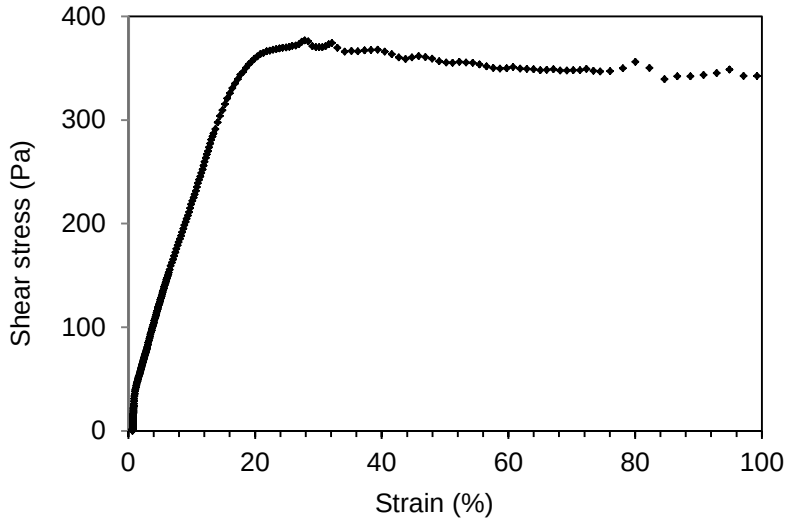

453
454 **Fig. 3. Shear stress as a function of shear strain for cement paste without SP and with a water to**
455 **cement ratio of 0.25 (ϕ=56%)**

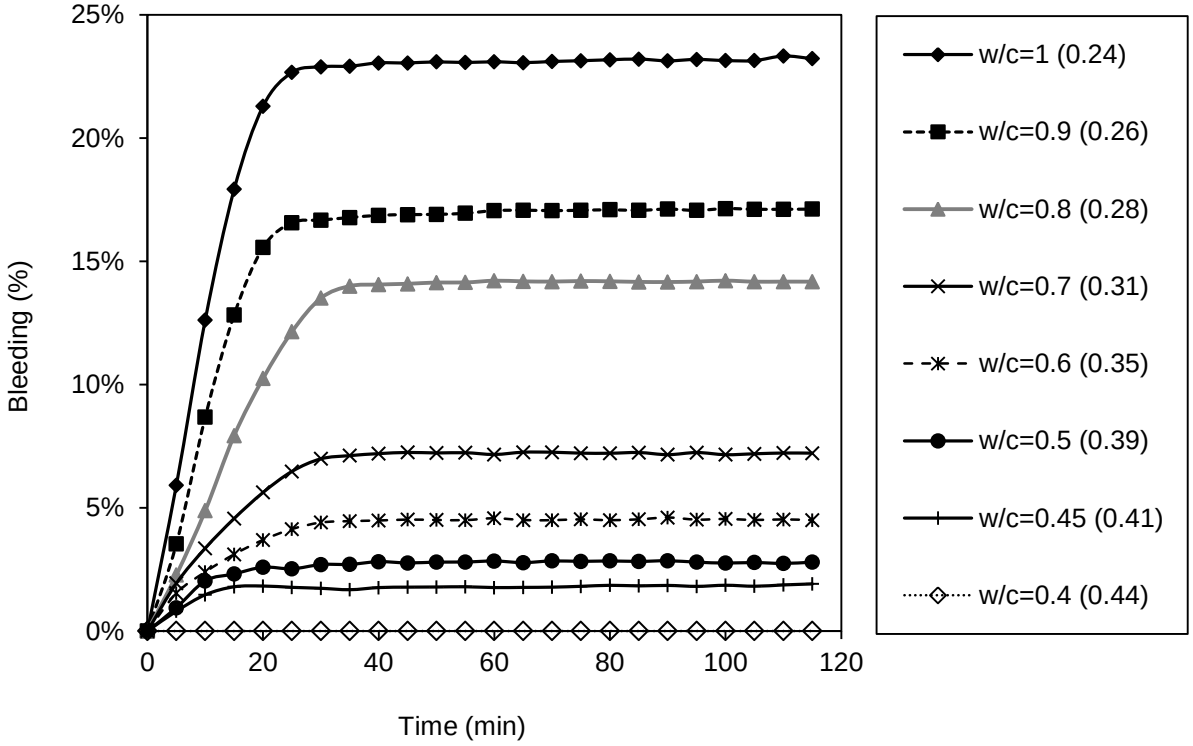

456
457 **Fig. 4. Evolution of bleeding as a function of water to cement ratio for cement pastes, in brackets is**
458 **the solid volume fraction**

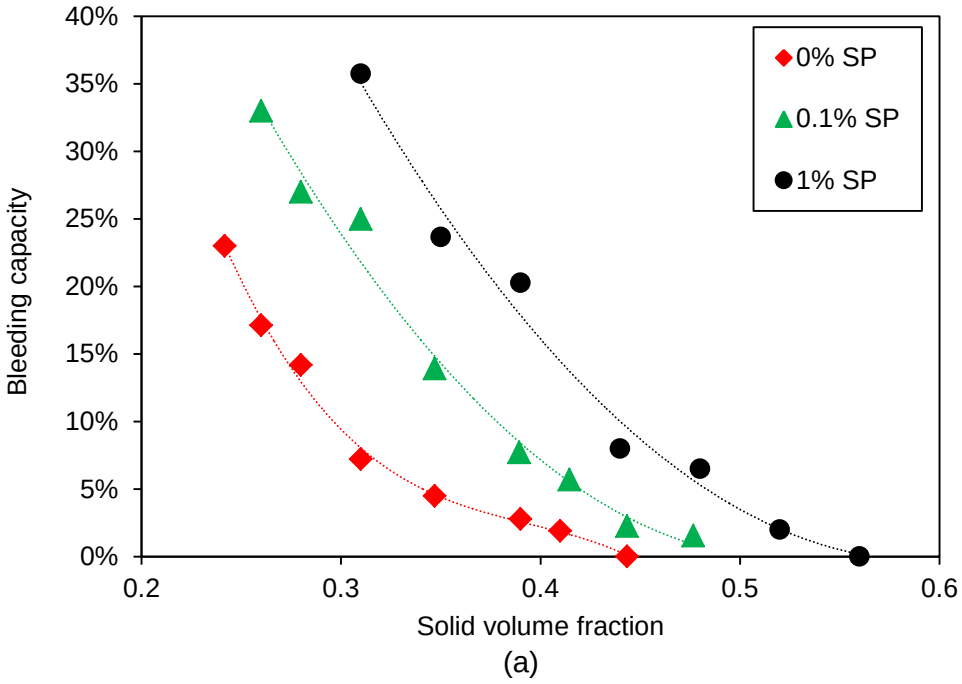

(a)

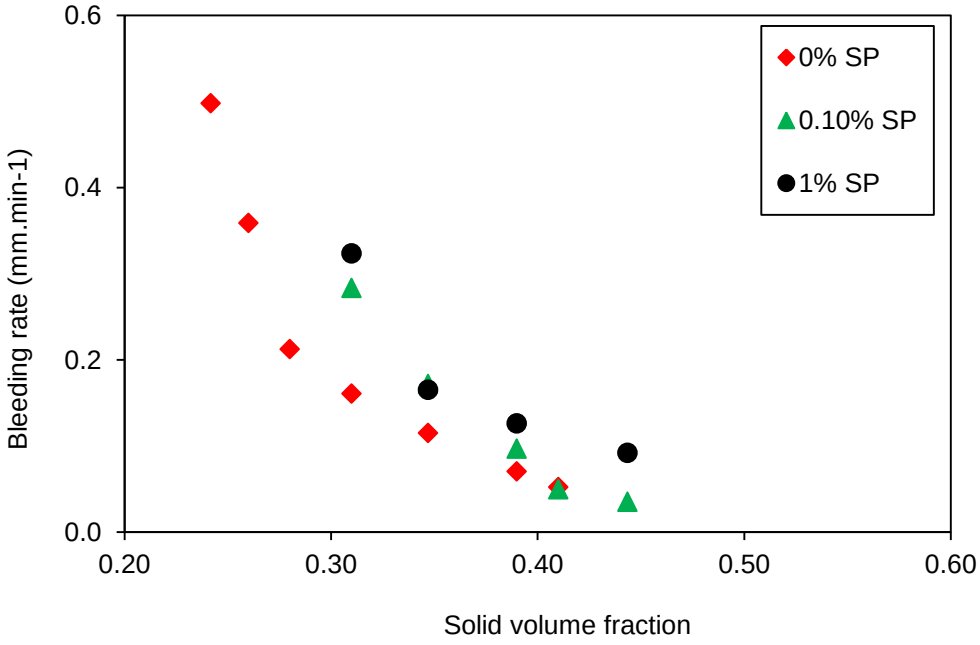

(b)

459 **Fig. 5. Bleeding capacity (a) and bleeding rate (b) as a function of solid volume fraction**
460
461

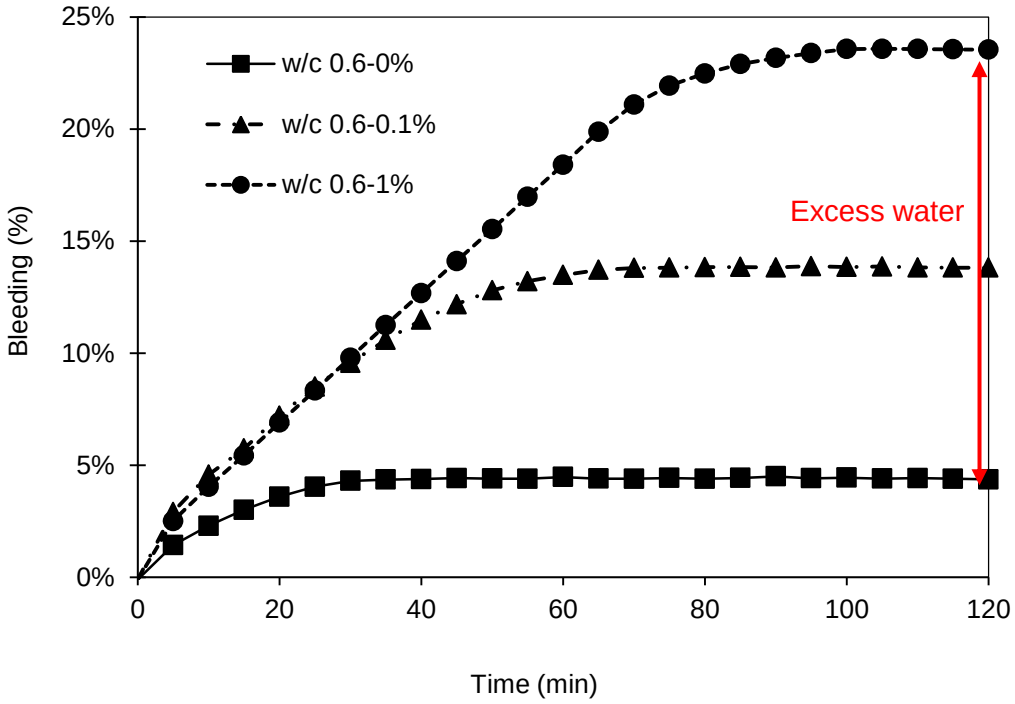

462
463
464 **Fig. 6. Evolution of bleeding for cement pastes with time for w/c ratio of 0.6 (solid volume fraction of 0.35)**

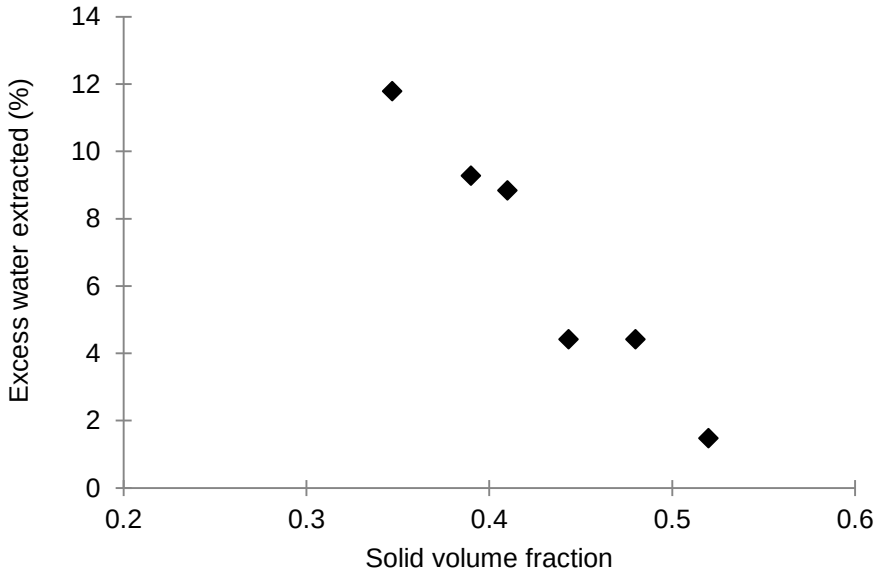

465
466 **Fig. 7. Excess water extracted as a function of solid volume fraction**

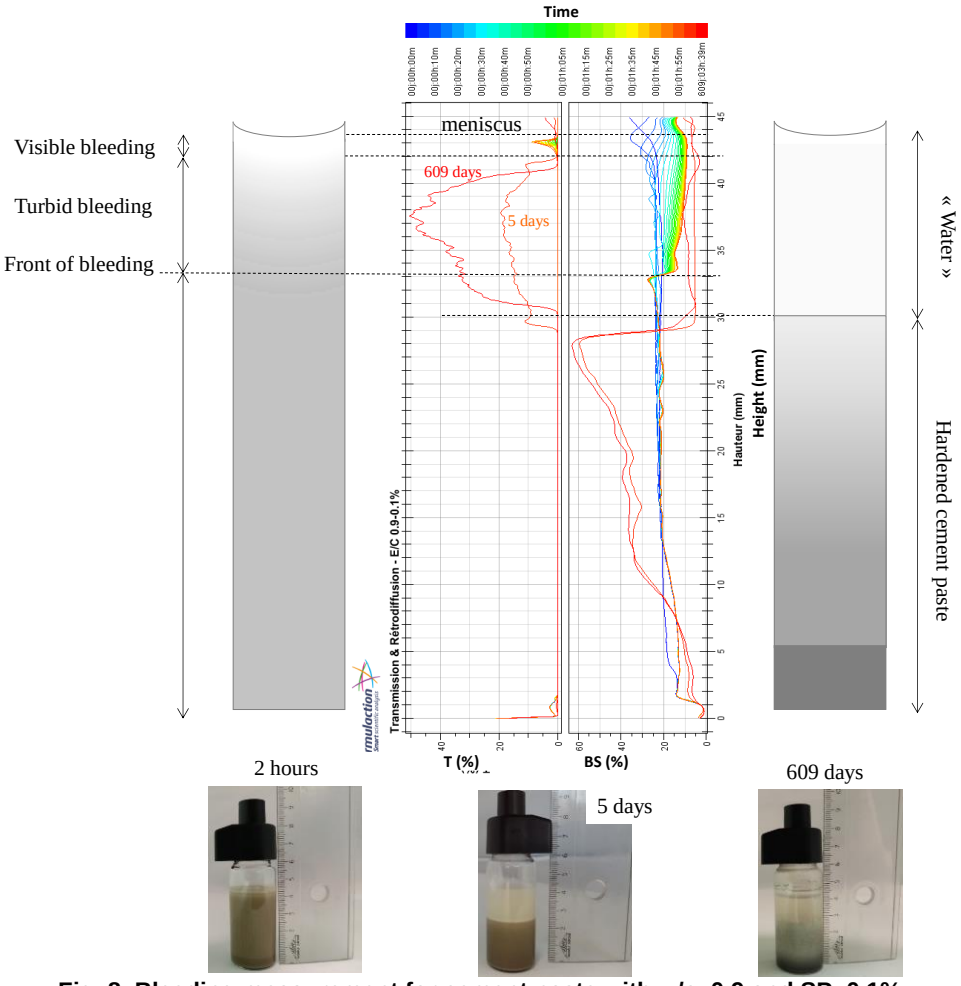

467
468

Fig. 8. Bleeding measurement for cement paste with w/c=0.9 and SP=0.1%

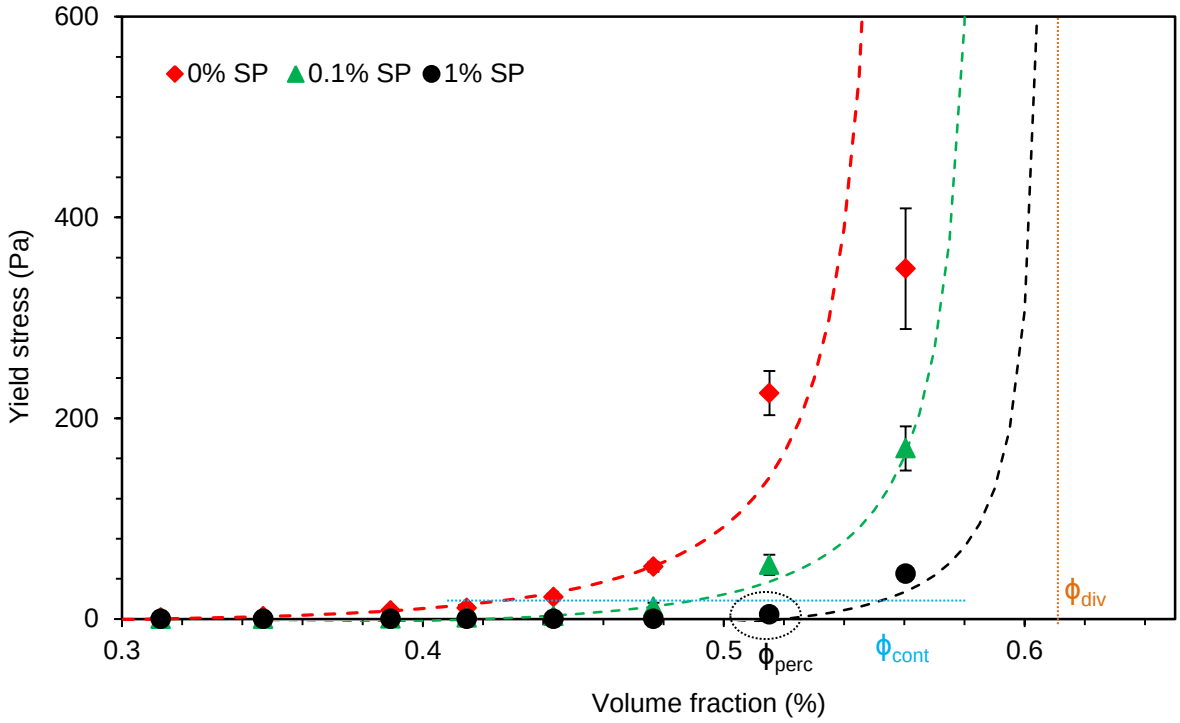

469

470 **Fig. 9. Yield stress as a function of solid volume fraction for cement paste containing 0, 0.1 and 1**
471 **wt% of PCE**

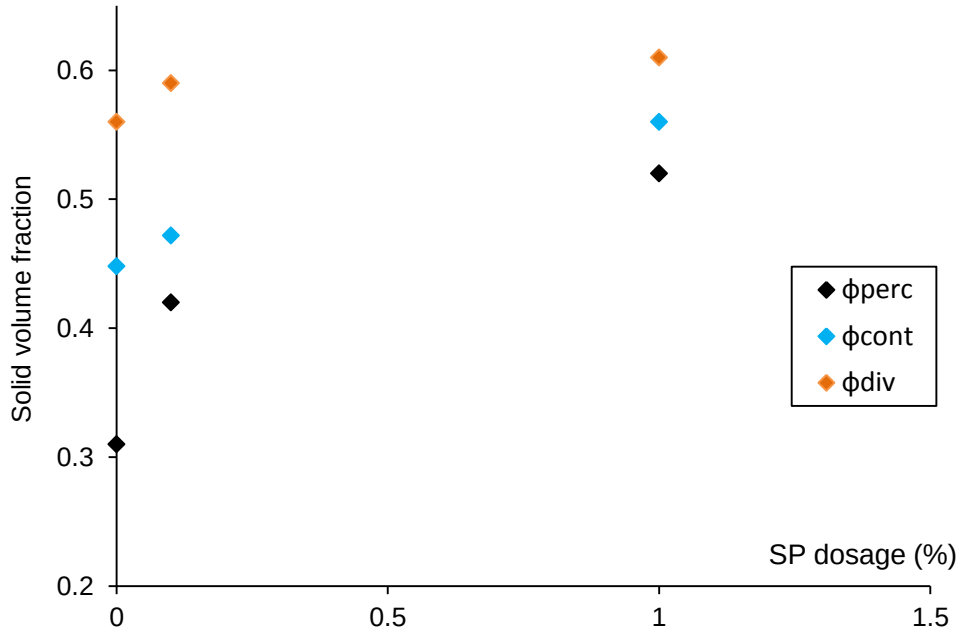

472
473 **Fig. 10. Transition volume fractions as a function of superplasticizer dosage**

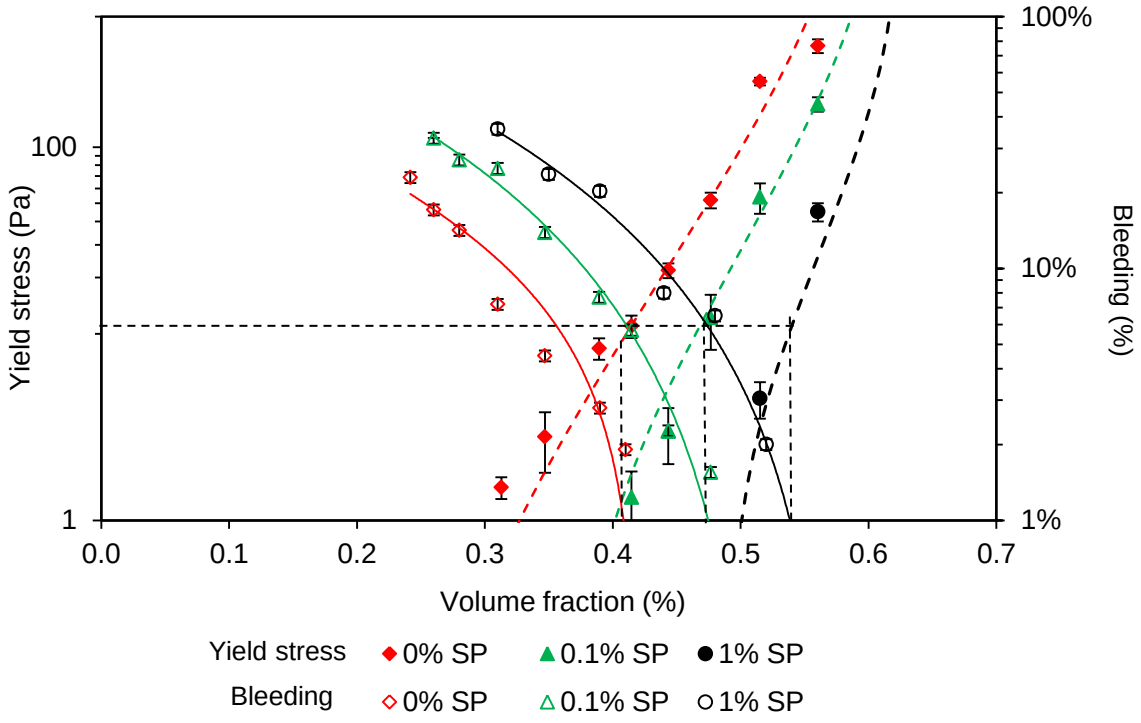

Fig. 11. Yield stress and bleeding as a function of solid volume fraction

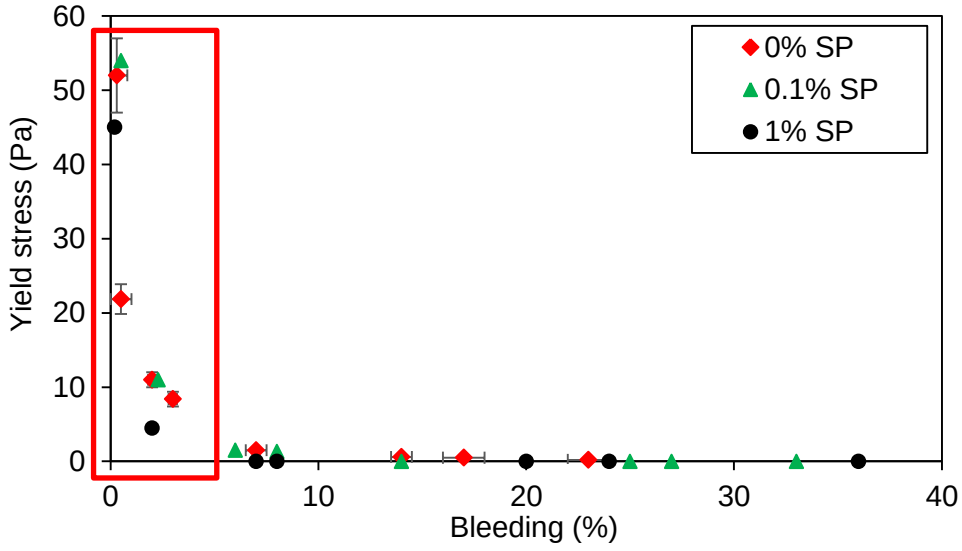

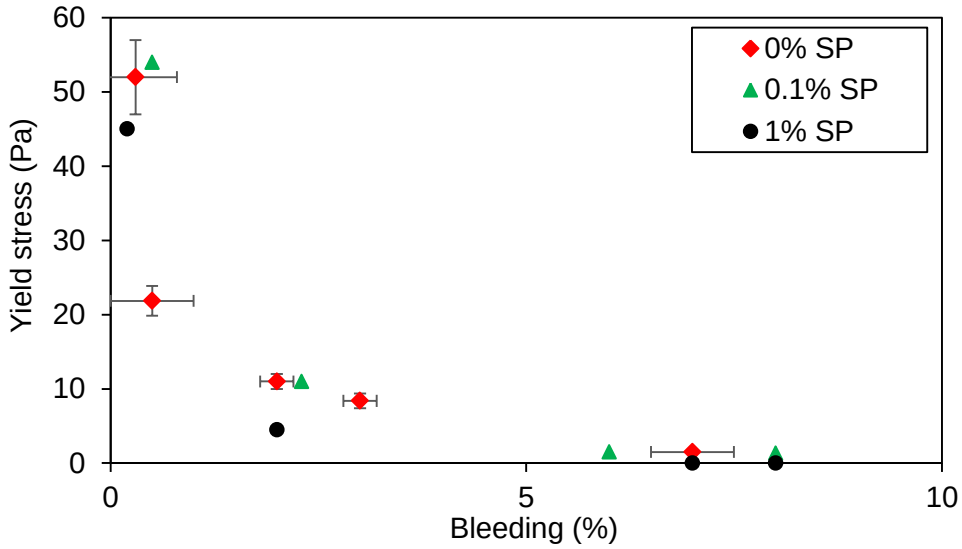

Fig. 12. Correlation between yield stress and bleeding

List of figures and tables

Fig. 24. Correlation between yield stress and bleeding